SCIENTIFIC REPORTS

OPEN

# High Sensitivity and Selectivity of AsP Sensor in Detecting $SF_6$ Decomposition Gases

Received: 8 May 2018
Accepted: 2 August 2018
Published online: 13 August 2018

Wang Jin[1], Yang Guofeng[2], Xue Junjun[3], Lei Jianming[1], Cai Qing[1], Chen Dunjun[1], Lu Hai[1], Zhang Rong[1] & Zheng Youdou[1]

**The sensing properties of monolayer arsenic phosphorus (AsP) for the adsorption of $SF_6$, $H_2O$, $O_2$, and $SF_6$ decomposition gases ($SO_2$ and $H_2S$) are theoretically investigated by the first-principle calculations. We calculate the adsorption energy, equilibrium distance, Mulliken charge transfer, and electron localization function (ELF) to explore whether AsP is suitable for detecting $SF_6$ decomposition gases. By comparing the adsorption performance of $SF_6$, $H_2O$, $O_2$, and $H_2S$ gases, we have revealed that the $SO_2$ gas molecules could form stable chemisorption with AsP monolayer. The results demonstrate that AsP is highly sensitive and selective to $SO_2$ gas molecules with robust adsorption energy and apparent charge transfer. Furthermore, the current-voltage (*I–V*) curves reveal that only the adsorption of $SO_2$ can largely modify the resistance of AsP. Our results show that gas sensors based on AsP monolayer could be better than that of black phosphorene (BP) to diagnose the state of online gas-insulated switchgear (GIS).**

Sulfur hexafluoride ($SF_6$) is widely used in gas-insulated switchgear (GIS) due to its excellent thermal conductivity, high dielectric strength, arc-extinguishing properties, and chemical inertness[1,2]. However, trace amounts of $O_2$ and $H_2O$ are unavoidable impurities in GIS[3]. With time going by, the internal insulation defects and aging in GIS equipment may cause partial discharge, which will decompose $SF_6$ into $SO_2$, $H_2S$, and other decomposition products[4,5]. These decomposition products will further accelerate insulation deterioration in GIS, and even affect the normal work of the electric equipment. Therefore, the online detection of the $SF_6$ decomposition gases in GIS is essential and significant to reduce unnecessary losses caused by the breakdown of GIS equipment. The sensing methods for $SF_6$ decomposition gases include gas chromatography, mass spectrometry, infrared (IR) spectroscopy, ion mobility spectrometry, and metal oxides sensors and so on[6–8]. However, these methods are not suitable for online detection because most of them require sophisticated instruments, well-trained operators, or special operating environment.

Gas sensors based on two-dimensional (2D) materials have drawn considerable attention due to their prominent advantages such as simple, cost-effective, and portable as well as high precision and sensitivity[9,10]. A lot of 2D materials, such as graphene, phosphorene, $MoTe_2$ and so on, have been applied to detect the $SF_6$ decomposition gases[11–13]. Arsenic phosphorus (AsP) monolayer, which is a phosphorene analogue formed from a 1:1 stoichiometric mixture of P and As. Surprisingly, the electron mobility of AsP monolayer along the armchair direction ($\sim 10000\, cm^2\, V^{-1}\, s^{-1}$) is 1 order of magnitude larger than that of the black phosphorene (BP)[14]. It's well known that higher carrier mobility is beneficial to gas sensor applications. More importantly, $As_xP_{1-x}$ ($x = 0 \sim 0.83$) was successfully synthesized recently by using alloying strategy[15]. It has been reported that Si-doped AsP displays an excellent sensitivity for $H_2S$ molecules[16]. However, there is no previous work reported whether monolayer AsP is suitable for detecting $SF_6$ decomposition gases. Therefore, we firstly investigate the sensing performances of AsP for detecting the main decomposition gases of $SF_6$ ($SO_2$ and $H_2S$) with consideration of the background gas ($SF_6$, $H_2O$, and $O_2$) by using First-Principles.

[1]Key Laboratory of Advanced Photonic and Electronic Materials, School of Electronic Science and Engineering, Nanjing University, Nanjing, 210093, China. [2]School of Science, Jiangsu Provincial Research Center of Light Industrial Optoelectronic Engineering and Technology, Jiangnan University, Wuxi, 214122, China. [3]School of Electronic Science and Engineering, Nanjing University of Posts and Telecommunications, Nanjing, 210023, China. Correspondence and requests for materials should be addressed to C.D.J. (email: djchen@nju.edu.cn)

| Molecule | $E_a$ (eV) | $d_0$ (Å) | $Q$ (e) |
|---|---|---|---|
| $SF_6$ | −0.480 | 3.09 (P-F) | −0.053 |
| $SO_2$ | −1.031 | 2.59 (P-S) | 0.151 |
| $H_2S$ | −0.069 | 3.07 (P-S) | −0.065 |
| $H_2O$ | −0.433 | 2.51 (P-H) | 0.012 |
| $O_2$ | −0.342 | 2.80 (P-O) | 0.013 |

**Table 1.** The Adsorption Energy, Equilibrium Distance, and Mulliken Charge Transfer of Different Molecules Adsorbed on Arsenic Phosphorus Monolayer.

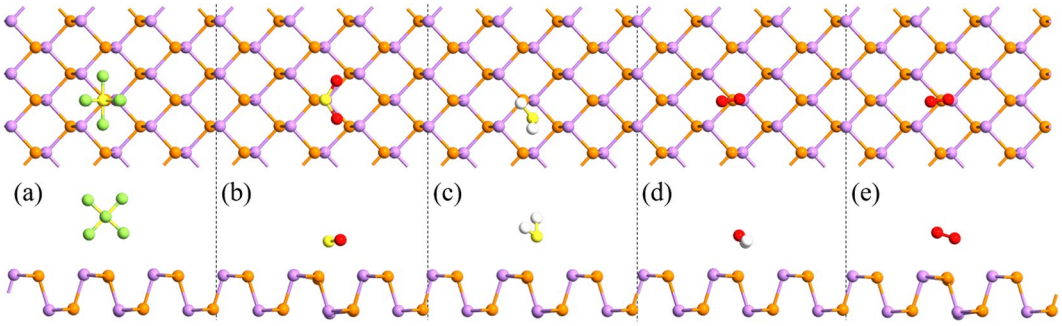


**Figure 1.** The top side views of the most stable adsorption structures of the small gas molecles: (**a**) $SF_6$, (**b**) $SO_2$, (**c**) $H_2S$, (**d**) $H_2O$ and (**e**) $O_2$ on monolayer AsP. (The purple and yellowish-brown balls represent As and P atoms, where yellow, green, red, and white represent S, F, O, H atoms, respectively).

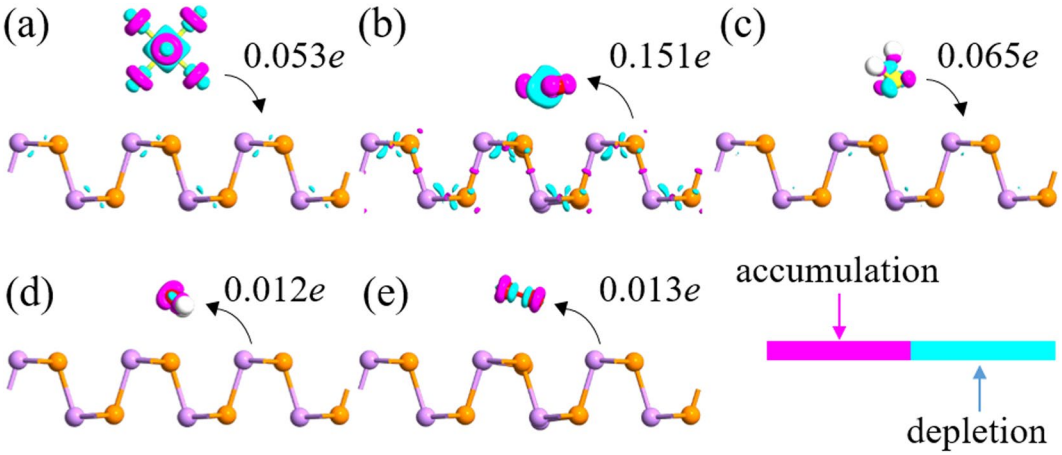


**Figure 2.** The side views of EDD calculation for (**a**) $SF_6$, (**b**) $SO_2$, (**c**) $H_2S$, (**d**) $H_2O$, and (**e**) $O_2$ adsorbed on the AsP monolayer. The isovalue is 0.17 au. The cyan and purple regions indicate electron depletion and accumulation, respectively. The direction of charge transfer is shown by the arrow.

## Results

The most stable configurations of the different gas molecules adsorption on AsP monolayer are illustrated in Fig. 1, and the corresponding $E_a$, $d_0$ and $Q$ are listed in Table 1. The positive sign of $Q$ means charge transfer from monolayer AsP to the adsorbates. As listed in Table 1, the equilibrium distance of $SF_6$, $SO_2$, $H_2S$, $H_2O$, and $O_2$ on the AsP monolayer (3.09, 2.59, 3.07, 2.51, and 2.80 Å, respectively) are larger than P-F (1.75 Å), P-S (2.14 Å), P-H (1.43 Å), and P-O (1.74 Å) bonds[17]. The $E_a$ of the most energetically favorable structures for $SF_6$, $SO_2$, $H_2S$, $H_2O$, and $O_2$ molecules adsorbed on AsP are −0.480, −1.031, −0.069, −0.433, and −0.342 eV, respectively. Clearly, the adsorption energy of $H_2S$ on AsP is significantly smaller than the others, indicating that the AsP monolayer is not suitable for sensing this molecule. The $E_a$ value of $SO_2$ adsorption on AsP monolayer is also larger than that of $SO_2$ adsorption on BP (−0.748 eV)[18], indicating that a higher level sensitivity for $SO_2$ detection with AsP than that with BP.

Charge transfer is another important factor to estimate the sensitivity of gas sensors. To further explore the adsorption properties between gas molecules and the AsP monolayer, the electron difference densities (EDD) are shown in Fig. 2. The Mulliken charge transfer results for $SF_6$/$H_2S$-AsP systems show that the charge is depleted

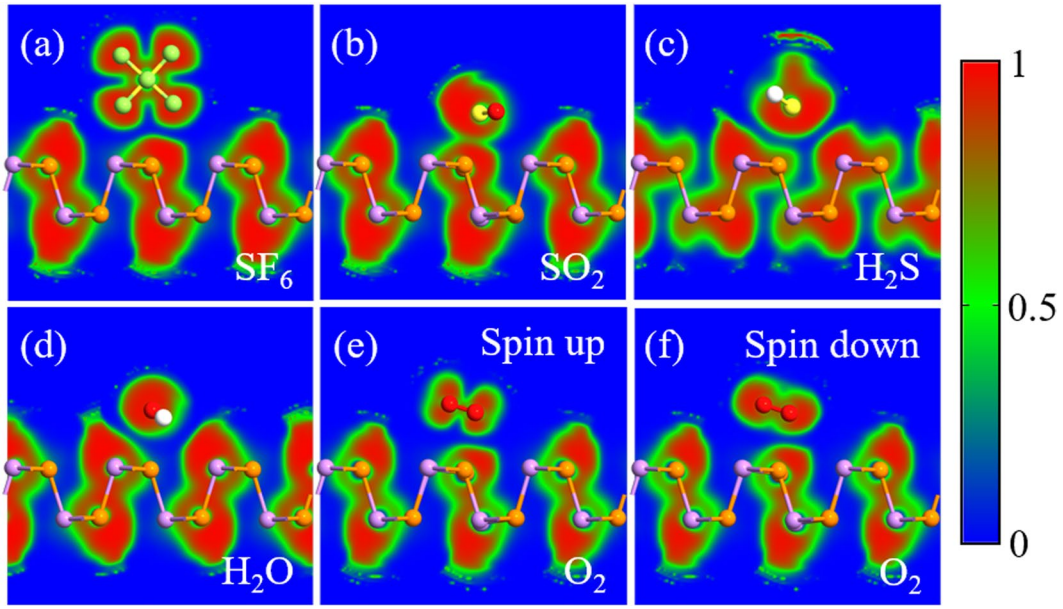


**Figure 3.** The side views of ELF calculation for (**a**) $SF_6$, (**b**) $SO_2$, (**c**) $H_2S$, (**d**) $H_2O$, and (**e**) $O_2$ spin up and (**f**) $O_2$ spin down adsorbed on the AsP monolayer.

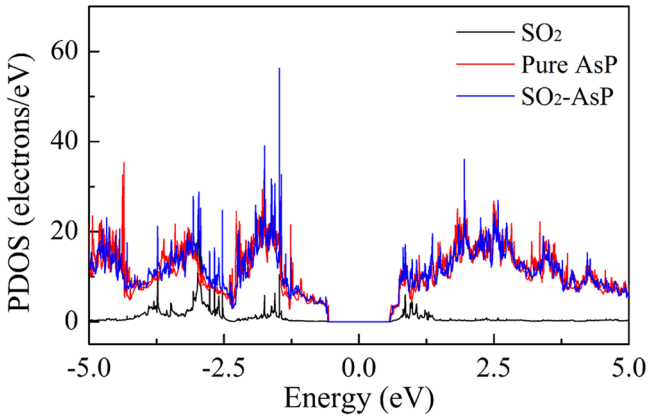


**Figure 4.** The total DOS of AsP with and without $SO_2$ adsorption and the PDOS of the $SO_2$ on the pure phosphorene.

on gas molecules and accumulated on the AsP surface, while the other three systems are exactly reversed. When $SF_6$ and $H_2S$ molecules are adsorbed on AsP surface, they usually act as charge donors and provide 0.053 and 0.065 *e* to the AsP monolayer, respectively. $H_2O$ and $O_2$ act as a charge acceptor and obtains 0.012 and 0.013 *e* from monolayer AsP. However, the charge transfer (*Q*) for these gas molecules is largely smaller than $SO_2$-AsP system (0.151 *e* transfer from AsP to $SO_2$ molecule). When we look into the EDD of $SO_2$-AsP system, a much more significant charge transfer is observed. These results indicate that the electrostatic interactions between $SF_6$/$H_2S$/$H_2O$/$O_2$-AsP systems are obviously weaker than $SO_2$-AsP system. Thus, the AsP monolayer is not suitable for detecting these four molecules.

To further obtain insight into the charge redistribution of the adsorption system, we plot the electron localization function (ELF) slices in Fig. 3. There is no obvious electron localization overlap between $SF_6$, $H_2S$, $H_2O$, and $O_2$ gas molecules and the AsP monolayer, which means the physisorption feature for these molecules adsorbed on AsP monolayer. The ELF of the $SF_6$-, $H_2S$-, $H_2O$-, and $O_2$-AsP systems do not have electron sharing area between gas molecules and the AsP monolayer, and thus the AsP monolayer is not sensitive to these molecules. For the $SO_2$-AsP system, the electrons are slightly shared between $SO_2$ molecule and AsP monolayer, revealing that the surface charge of the AsP monolayer is largely redistributed after $SO_2$ adsorption. This is consistent with the result of the Mulliken charge transfer. For $SO_2$ adsorption, it would be more reasonable to treat it as chemisorption due to the large binding energy, electron transfer and also slightly overlapped electron distribution as shown in Fig. 3(b). To further explore the adsorption mechanisms of $SO_2$ molecules adsorbed on AsP monolayer, we plot the total electronic densities of states (DOS) and projected density of states (PDOS) in Fig. 4. Obviously, the main

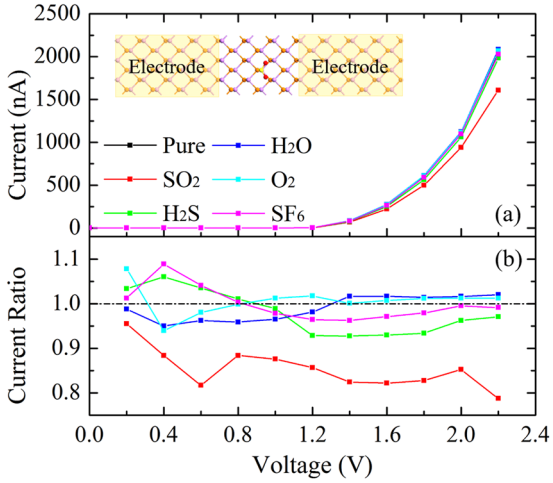


**Figure 5.** (**a**) The current-voltage (*I*–*V*) curves along the armchair direction of AsP monolayer before and after $SO_2$, $H_2S$, $H_2O$, $O_2$ and $SF_6$ adsorption. The inset is the top view of the two-probe system of AsP monolayer with $SO_2$ adsorption. (**b**) Current ratios of the two-probe systems with and without gas molecule adsorption.

electronic level contributions of $SO_2$ to the total system localize between −4 and −1.3 eV in the valence band, 1 and 1.3 eV in the conduction band, which is away from the Fermi level. The electrons are slightly shared between AsP monolayer and $SO_2$ molecule, which reveals the intensity of the interaction between the $SO_2$ molecule and the AsP monolayer. These findings imply that the strong adsorption of $SO_2$ on AsP monolayer is mostly due to the electron Coulomb interaction between the lonely paired electrons of $SO_2$ and the empty orbital of P atom, without hybridization[19]. Thus, we can deduce that gas sensors based on AsP are sensitive and selective to $SO_2$ gas in the background of the $SF_6$ decomposition gases.

To further verify the validity of our work, we calculate the *I*–*V* response of AsP sensor before and after the gas adsorption, as shown in Fig. 5(a). Armchair direction is chosen for transport calculation because the mobility along the armchair direction is significantly larger than the zigzag direction. There is no current (about 0.1 nA) passing through the devices when the bias voltage is smaller than 1.0 V due to the existence of band gap of pure AsP. When bias over 1.0 V, the current starts to increase dramatically. However, for the $SO_2$ adsorption, with the increase of the bias voltage from 1.2 to 2.2 V, the current is clearly smaller than other cases. The reduction of current indicates the resistance of AsP is increased after the $SO_2$ adsorption, which can be easily measured in the experiment. It should be emphasized that the increased resistance is caused by the larger charge transfer between the AsP monolayer and $SO_2$ molecule. To gain deeper insight into the resistance change of AsP caused by the different adsorbates, we plot the current ratios before and after adsorption of gas in Fig. 5(b). It can be found that the current ratios for $SO_2$ adsorption are significantly lower than that for $H_2S$ and $SF_6$ adsorption. The value of the current reduction is about 21.3% for $SO_2$ adsorption under a bias of 2.2 V, while the current reductions are 2.9% and 0.8% for $H_2S$ and $SF_6$ adsorption respectively under the same bias. The current reduction ratio for $SO_2$ adsorption is about seven times as that for $H_2S$ and $SF_6$ adsorption, which can be easily distinguished by the magnification. The current is slightly enhanced after the $H_2O$ and $O_2$ adsorption under a bias of 2.2 V. The resistance in AsP monolayer is highly selective and sensitive to $SO_2$ in $SF_6$ decomposition gases, which further demonstrates that it can be an excellent sensing material for online GIS diagnosis.

## Discussion

It was reported that BP could also be used for $SO_2$ gas detection in $SF_6$ decomposition gases[11]. However, the maximum current reduction is about 7% for $SO_2$ adsorption, and not more than 1.5% for $H_2S$ and $SF_6$ adsorption. For comparison purposes, we estimate the sensor response (*S*) with the formula:

$$S(\%) = \Delta R/R \times 100\%,$$

where $\Delta R$ is the resistance change after $SO_2$ adsorption and *R* is the prior resistance of AsP monolayer. It should be emphasized that it is different to compare *S* directly in experiments because the sensitivities of 2D materials are affected by many factors, such as their thicknesses, detecting areas and so on. Nonetheless, our AsP sensor shows better response to $SO_2$ than BP in the theoretical calculations, indicating that AsP monolayer could do better than BP in fabricating high sensitivity $SO_2$ sensors for application in online GIS diagnosis, at least comparable to BP.

## Methods

The first principles calculations based on density functional theory (DFT) are performed using the Atomistix Tool Kit (ATK) codes at room temperature (T = 300 K)[20]. The generalized gradient approximation (GGA) with Perdew-Burke-Ernzerhof (PBE) exchange-correlation potential is adopted[21]. Fritz Haber Institute (FHI) pseudopotential using Troullier-Martins scheme with a double-ζ basis set is employed[22]. Spin polarization is only included during the calculations of the adsorption of $O_2$ because it is a paramagnetic molecule. We use the Grimme's DFT-D2 dispersion correction approach for van der Waals (vdW) corrections thanks for its higher

accuracy[23]. The vacuum region is set to more than 15 Å to avoid the effect of interaction springing from the adjacent layers. A well conserved Monkhorst-Pack $8 \times 8 \times 1$ k-point mesh is adopted for geometry optimization and electronic properties calculations with a density mesh cutoff energy of 300 Ry. Previously reported optimized lattice constants for monolayer AsP (a = 3.5 Å and b = 4.65 Å) are considered in this work[14]. We take a $3 \times 3$ supercell of monolayer AsP. The current-voltage ($I$–$V$) characteristics are calculated by using the nonequilibrium Green's function (NEGF) method[24]. The k-point sampling is set to $5 \times 1 \times 100$, and the mesh cutoff is set to 200 Ry for $I$–$V$ calculation. The current of two-probe systems are calculated by the Landauer–Bütiker formula:

$$I = \int_{-\infty}^{+\infty} T(E, V_b)[f_l(E - u_l) - f_r(E - u_r)]dE \quad (1)$$

where $T(E, V_b)$ is the electron transport coefficient calculated from the Green's functions, $f$ and $u$ are the Fermi-Dirac distribution function and the electrochemical potential, respectively. The subscripts "$r$" and "$l$" represent the right and left electrode.

To find the most stable configurations, we consider four different sites for each gas adsorbed on monolayer AsP, which are set up at the top of upper As/P atom, the middle of As-P bond, and the center of the puckered hexagon. The moderate distance (2.5 Å) between a single molecule and monolayer AsP layer is adopted for each initial adsorption case. On the basis of the above settings, all the configurations are fully optimized and relaxed until the force and stress tolerance are mitigated to less than 0.05 eV/Å and 0.001 eV/Å$^3$, respectively. To study the interactions between monolayer AsP and targeted gas molecules, the adsorption energy ($E_a$), the Mulliken charge transfer ($Q$) and the adsorption distance ($d_0$) are systematically calculated. The adsorption energy is defined as:

$$E_a = E_{total} - E_{gas} - E_{AsP}$$

where $E_{gas}$, $E_{AsP}$, and $E_{total}$ are the total energy of gas molecule, AsP monolayer, and gas molecule-AsP system, respectively. The adsorption distance is defined as the equilibrium's nearest atoms between AsP monolayer and gas molecules.

## Conclusion

In conclusion, we have investigated the sensing properties of AsP monolayer for two main $SF_6$ decomposition gas molecules ($SO_2$, $H_2S$) and three background gas molecules ($SF_6$, $H_2O$, and $O_2$) adsorption by using the first-principles calculations. The results demonstrate that $SF_6$, $H_2S$, $H_2O$, and $O_2$ gas molecules show physical adsorption on AsP monolayer, while AsP monolayer strongly adsorb $SO_2$ molecules via robust chemical bonds. It is found that the $E_a$ and $Q$ values of $SO_2$ molecule adsorbed on AsP monolayer are obviously larger than the others, which may allow it as a desirable gas sensor for detecting $SO_2$. The $I$–$V$ curves demonstrate that the resistance of AsP monolayer is only largely affected by $SO_2$ adsorption, indicating that the gas sensors based on AsP are highly sensitive and selective to $SO_2$. Therefore, we can deduce that AsP is a promising candidate for high sensitivity and selectivity $SO_2$ sensing applications in online GIS diagnosis for $SF_6$ decomposition gases.

## References


1. Kim, K. H., Ingole, P. G., Kim, J. H. & Lee, H. K. Experimental investigation and simulation of hollow fiber membrane process for $SF_6$ recovery from GIS. *Polym. Adv. Technol.* **24**, 997–1004 (2013).
2. Cai, T., Wang, X.-P., Huang Yun, G. & Du Shuang, Y. Infrared Spectrum Analysis of $SF_6$ and $SF_6$ Decomposition. *Spectroscopy and Spectral Analysis* **30**, 2967–2970 (2010).
3. Fu, Y. *et al.* Theoretical study of the neutral decomposition of $SF_6$ in the presence of $H_2O$ and $O_2$ in discharges in power equipment. *Journal of Physics D-Applied Physics* **49** (2016).
4. Beyer, C., Jenett, H. & Klockow, D. Influence of reactive SFx gases on electrode surfaces after electrical discharges under $SF_6$ atmosphere. *Ieee Transactions on Dielectrics and Electrical Insulation* **7**, 234–240 (2000).
5. Chu, F. Y. SF6 Decomposition in Gas-Insulated Equipment. *Ieee Transactions on Electrical Insulation* **21**, 693–725 (1986).
6. Dong, M., Zhang, C., Ren, M., Albarracin, R. & Ye, R. Electrochemical and Infrared Absorption Spectroscopy Detection of $SF_6$ Decomposition Products. *Sensors* **17** (2017).
7. Zhang, X., Tian, S., Xiao, S., Huang, Y. & Liu, F. Partial Discharge Decomposition Characteristics of Typical Defects in the Gas Chamber of $SF_6$ Insulated Ring Network Cabinet. *Ieee Transactions on Dielectrics and Electrical Insulation* **24**, 1794–1801 (2017).
8. Zhang, X., Zhang, J., Jia, Y., Xiao, P. & Tang, J. $TiO_2$ Nanotube Array Sensor for Detecting the $SF_6$ Decomposition Product $SO_2$. *Sensors* **12**, 3302–3313 (2012).
9. Wang, J. *et al.* A Reusable and High Sensitivity Nitrogen Dioxide Sensor Based on Monolayer SnSe. *Ieee Electron Device Letters* **39**, 599–602 (2018).
10. Lee, S. W., Lee, W., Hong, Y., Lee, G. & Yoon, D. S. Recent advances in carbon material-based $NO_2$ gas sensors. *Sensors and Actuators B-Chemical* **255**, 1788–1804 (2018).
11. Yang, A.-J. *et al.* Phosphorene: A Promising Candidate for Highly Sensitive and Selective $SF_6$ Decomposition Gas Sensors. *Ieee Electron Device Letters* **38**, 963–966 (2017).
12. Wang, D.-W. *et al.* MoTe2: A Promising Candidate for $SF_6$ Decomposition Gas Sensors With High Sensitivity and Selectivity. *Ieee Electron Device Letters* **39**, 292–295 (2018).
13. Zhang, X., Yu, L., Wu, X. & Hu, W. Experimental Sensing and Density Functional Theory Study of $H_2S$ and $SOF_2$ Adsorption on Au-Modified Graphene. *Advanced Science* **2** (2015).
14. Shojaei, F. & Kang, H. S. Electronic Structure and Carrier Mobility of Two-Dimensional alpha Arsenic Phosphide. *Journal of Physical Chemistry C* **119**, 20210–20216 (2015).
15. Liu, B. *et al.* Black Arsenic-Phosphorus: Layered Anisotropic Infrared Semiconductors with Highly Tunable Compositions and Properties. *Adv. Mater.* **27**, 4423–4429 (2015).
16. Zhang, Y., Tan, C., Yang, Q., Ye, H. & Chen, X.-P. Arsenic Phosphorus Monolayer: A Promising Candidate for $H_2S$ Sensor and NO Degradation With High Sensitivity and Selectivity. *Ieee Electron Device Letters* **38**, 1321–1324 (2017).
17. Pyykko, P. & Atsumi, M. Molecular Single-Bond Covalent Radii for Elements 1–118. *Chemistry-a European Journal* **15**, 186–197 (2009).
18. Yang, Q. *et al.* First-Principles Study of Sulfur Dioxide Sensor Based on Phosphorenes. *Ieee Electron Device Letters* **37**, 660–662 (2016).

19. Dong, H., Wang, L., Zhou, L., Hou, T. & Li, Y. Theoretical investigations on novel SiC5 siligraphene as gas sensor for air pollutants. *Carbon* **113**, 114–121 (2017).
20. Soler, J. M. *et al*. The SIESTA method for ab initio order-N materials simulation. *Journal of Physics-Condensed Matter* **14**, 2745–2779 (2002).
21. Perdew, J. P., Burke, K. & Ernzerhof, M. Generalized gradient approximation made simple. *Phys. Rev. Lett.* **77**, 3865–3868 (1996).
22. Blum, V. *et al*. Ab initio molecular simulations with numeric atom-centered orbitals. *Comput. Phys. Commun.* **180**, 2175–2196 (2009).
23. Grimme, S., Antony, J., Ehrlich, S. & Krieg, H. A consistent and accurate ab initio parametrization of density functional dispersion correction (DFT-D) for the 94 elements H-Pu. *J. Chem. Phys.* **132** (2010).
24. Brandbyge, M., Mozos, J. L., Ordejon, P., Taylor, J. & Stokbro, K. Density-functional method for nonequilibrium electron transport. *Physical Review B* **65** (2002).

## Acknowledgements

This work was supported by the National Key R&D Program of China (2017YFB0402900), the Key Project of Jiangsu Province, China (Grant No. BE2016174), the National Science Foundation of China (No. 61634002, 11604124 and 61604080), the Natural Science Foundation of Jiangsu Province (No. BK20150158 and BK20160883), the Fundamental Research Funds for Central Universities (No. JUSRP51628B), and the Postgraduate Research & Practice Innovation Program of Jiangsu Province (No. KYCX18_0030).

## Author Contributions

C.D.J., L.H., Z.R. and Z.Y.D. conceptualized the study, W.J., Y.G.F., X.J.J. and C.Q. calculated the data and W.J., L.J.M. and C.D.J. wrote the main manuscript text.

## Additional Information

**Competing Interests:** The authors declare no competing interests.

**Publisher's note:** Springer Nature remains neutral with regard to jurisdictional claims in published maps and institutional affiliations.